3D-Printed Compact Bandpass Filters Based on Conical Posts

Enrique López-Oliver, Cristiano Tomassoni, *Senior, IEEE,* Lorenzo Silvestri, *Member, IEEE,* Maurizio Bozzi, *Fellow, IEEE,* Luca Perregrini, *Fellow, IEEE,* Stefania Marconi, Gianluca Alaimo, and Ferdinando Auricchio

***Abstract*—This paper presents different physical arrangements of filters using conical posts as the basic element of design. The proposed resonator is similar to that of the classical combline filter, however, in this case, a conical post (truncated cone) is exploited. A hollowed enclosure is positioned on top of a rectangular metallic cavity for housing the upper part of the conical resonating post. Considering that the post upper radius is smaller than the post lower radius, an enclosure having the same dimensions as the resonating post can be taken. This results in a housing that can also work as a resonator for another cavity. As a result, cavities can be piled in a vertical arrangement and the conical post of each cavity is also used as housing for the post of the cavity below it. Mixed vertically and/or horizontally arrangements are also feasible. More compact structures can be achieved with the possibility to obtain different footprints while maintaining similar unloaded Q-factors than conventional combline filters. The structure also has the advantage of having a wider spurious-free range than the classical combline filter configuration (cylindrical post inside a rectangular cavity). Enhanced responses with higher rejections are also possible thanks to the introduction of transmission zeros. Several different filter configurations are presented in this paper: 3-order filter and 4-order filter. The design procedure is explained for both of them. A 4-order filter has been manufactured using additive manufacturing techniques and measured in order to validate the proposed structure.**

***Index Terms*—Additive manufacturing, 3D printing, bandpass filter, conical resonator, combline filter.**

I. Introduction

IN the last years, the number of communication devices is increased. An exponential increment is also forecast for the next years. Indeed, in the future also machines will be integrated into the communication system that was traditionally reserved for humans. With the internet of things (IoT), an increasing number of objects will communicate through the network. In this context, the development of low-cost and flexible technology is of capital importance. Reduction of mass and dimensions is also an important aspect for portability requirements. It is also very important for aerospace applications where performance matters. From the point of view of the performance, waveguide technology offers the best results, but at the expense of being a bulky technology. For this reason, in the last years, a lot of effort has been devoted to the reduction of dimensions and mass in waveguide devices. This is particularly important for filters, being the largest and heaviest components in a transceiver (except perhaps antennas).

One of the most important and popular solutions adopted to reduce the filter size is the use of dual-mode [1] or multi-mode [2] cavities. TM-mode cavity filters in both single- [3] and dual-mode configurations [4]–[6] have been introduced in order to shrink the filter length. The use of high permittivity dielectric material allows for a significant reduction of the filter dimensions while maintaining very good performance in terms of losses [7]–[14] and thermal stability [13]. Another classical way used for size reduction, is to use a metal post inside a cavity. This allows for the excitation of resonant TEM modes with a noticeable resonator size reduction that is paid with a (moderate) decreasing of the Q-factor. Resonant posts are exploited in combline filters [15], which are commonly used in radio base-stations for working frequencies below 3 GHz. This type of filters are often designed in a folded configuration [16] in order to allow couplings between non-adjacent cavities, thus generating transmission zeros (TZs). However, in several applications, inline configurations are needed, with the inconvenience of implementing TZs by creating multipaths between non-adjacent resonators. To overcome this problem, in [17] is presented a triplet, consisting of adjacent posts orthogonally positioned with respect to each adjacent resonator in order to allow a direct coupling between the first and the third post bypassing the second one. A direct coupling between the first and the second post, as well as between the first and the third post can be controlled thanks to a small metal plate. The same idea is also applied in [18], where the coupling between adjacent posts is obtained by a coupling screw. Similarly, in [19], posts are arranged in a cylindrical waveguide for obtaining an improvement in the control of couplings by using the post rotation angles. Another way to obtain TZs in an inline configuration is presented in [20] and [21]. The first and the second resonance of a couple of strongly coupled posts in an evanescent [20] and in a propagating

Manuscript received July 21, 2020; revised September 12, 2020. This work was supported by funds from the European Union's Horizon 2020 research and innovation programme under the Marie Skłodowska-Curie grant agreement No 811232. This article is an expanded version from the IEEE MTT-S International Microwave Symposium (IMS 2020), Los Angeles, CA, USA, August 4 - 6, 2020. *(Corresponding author: Enrique López-Oliver.)*

E. López-Oliver and C. Tomassoni are with the Department of Engineering, University of Perugia, 06123 Perugia, Italy (e-mail: enrique.lopezoliver@unipg.it; cristiano.tomassoni@unipg.it).

L. Silvestri, M. Bozzi and L. Perregrini are with the Department of Electrical, Computer and Biomedical Engineering, University of Pavia, 27100 Pavia, Italy (e-mail: lorenzo.silvestri01@ateneopv.it; maurizio.bozzi@unipv.it; luca.perregrini@unipv.it).

S. Marconi, G. Alaimo and F. Auricchio are with the Department of Civil Engineering and Architecture, University of Pavia, 27100 Pavia, Italy (e-mail: stefania.marconi@unipv.it; gianluca.alaimo01@ateneopv.it; auricchio@unipv.it).

[21] waveguide have been exploited as non-resonating and resonant modes, respectively, for obtaining a singlet capable of a pole and a transmission zero (TZ). Furthermore, posts with non-conventional geometries have also been exploited for increasing performances. The cup of mushroom-shaped posts, was used for increasing the capacitive load of the post, thus decreasing size and increasing the spurious-free band [22]. In that case, the filter was manufactured with the classical milling technique. However, when geometries become more complex, the classical milling technique can be inadequate. In such circumstances, the use of additive manufacturing (AM) techniques can be more advantageous. This is the case of [23], where mushroom shaped resonators are created and connected through metal bars for obtaining control over the generated TZs. The flexibility of AM has also been used in [24] to give a non-conventional shape to the cup of mushroom-shaped posts, thus obtaining a mixed inductive/capacitive coupling to implement TZs in an inline configuration while saving volume. Another way to save volume is to use a post higher than the cavity. In order to allow the post to stay in the cavity, a small cylindrical cavity is added on top of the rectangular cavity for housing part of the post exceeding the rectangular cavity height. In [25], that cylindrical housing has been used as an additional resonant post of another cavity positioned on top of the first cavity. Of course, the post of the second cavity has a larger diameter than that of the first. For this reason, it has been used for generating a second band. The resulting structure is a dual-band filter in which cavities positioned on the bottom generate the first band, and cavities positioned on the top generate the second band. In [26], the same configuration has been used with conical (truncated cone) posts. The shape of the conical posts allow for a conical enclosure on top of the cavity. As a result, the conical housing can have the same dimensions as the conical post that covers. This means that cavities on the bottom and cavities on the top have posts with the same dimensions and resonate at the same frequency. The feasibility of the proposed structure was demonstrated with the design of a 2-pole filter.

In this paper, the idea presented in [26] has been further developed and extended. New diagrams are presented and used in the design of higher order filters. An accurate comparison with classical combline filters is presented from the point of view of the Q-factor, volume occupation, and spurious-free band. Volume reduction and increased spurious-free band are demonstrated. Different filter arrangements, including mixed vertical/horizontal cavity distributions are shown. Different ways for the positioning of tuning screws have also been studied and reported in this paper. Finally, structures capable of negative couplings are presented and the way to use them for obtaining responses with TZs is shown.

II. Conical Resonator

Fig. 1 shows the physical configuration of the proposed resonator. It consists of a truncated cone shape with two different radii inside a rectangular metal cavity that has a hollowed conical cavity on top of it, working as a housing enclosure for the upper part of the resonating post. As will be shown later, the advantage of this structure is that the housing can be used as the conical resonant post of an additional cavity. The electric field distribution (E-field) of the resonant mode is similar to that of the combline resonator, a TEM mode in the transversal section of the resonator. However, due to the close gap between the conical housing and the conical post, a capacitive effect with the relevant field concentration is created, as shown in Fig. 1.

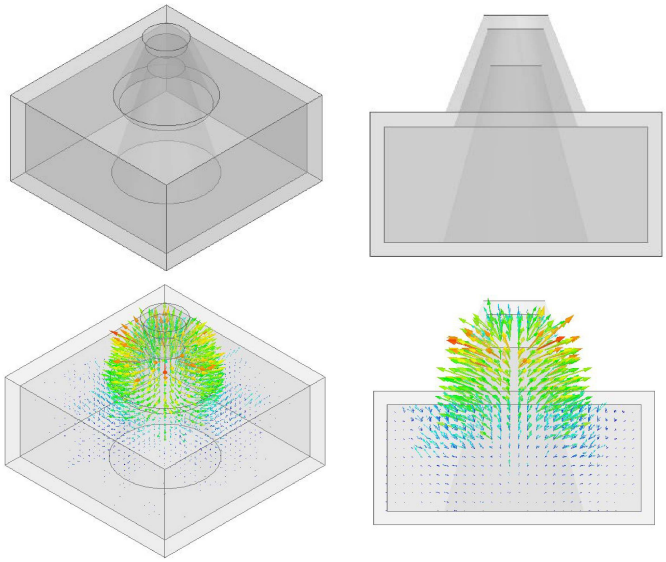

Fig. 1. 3D views of the proposed conical resonator with and without the electric field distribution.

Unlike the combline resonator, where the analysis can be carried out considering an equivalent circuit formed by a short-circuited transmission line ended with a capacitor, the presented structure cannot be easily analytically modeled because of its non-uniformity along the transverse section. For this reason, the analysis has been performed using the commercial software ANSYS High-Frequency Structure Simulator (HFSS). The analysis has been used for determining which physical parameters are more critical, and for optimizing the structure in terms of Q-factor and volume.

Fig. 2 encompasses various graphs showing the Q-factor and the resonance frequency of the first and second modes versus the physical parameters depicted in Fig. 3. Consequently, when looking for compactness, an option is to decrease the height of the cavity (h_{cav}). Decreasing h_{cav}, the resonating post is inserted more inside the housing enclosure, and, as can be seen from Fig. 2, the unloaded Q-factor (Q_u) and the first resonance decrease, while the second resonance increases. One way to compensate the decay of the Q_u is by decreasing the upper diameter (d_{ucone}), but also increasing the lower diameter (d_{lcone}) of the post. It is worth mentioning that the frequency of the second mode remains constant from one value of the lower diameter d_{lcone}, this can be considered as a starting point value if looking for a trade-off between Q-factor and the frequency of the second mode. The upper diameter (d_{ucone}), on the other hand, changes differently than d_{lcone}, except for the second resonance frequency that varies in the same way. Other variables such as the internal diameter (d_{cav}), or the

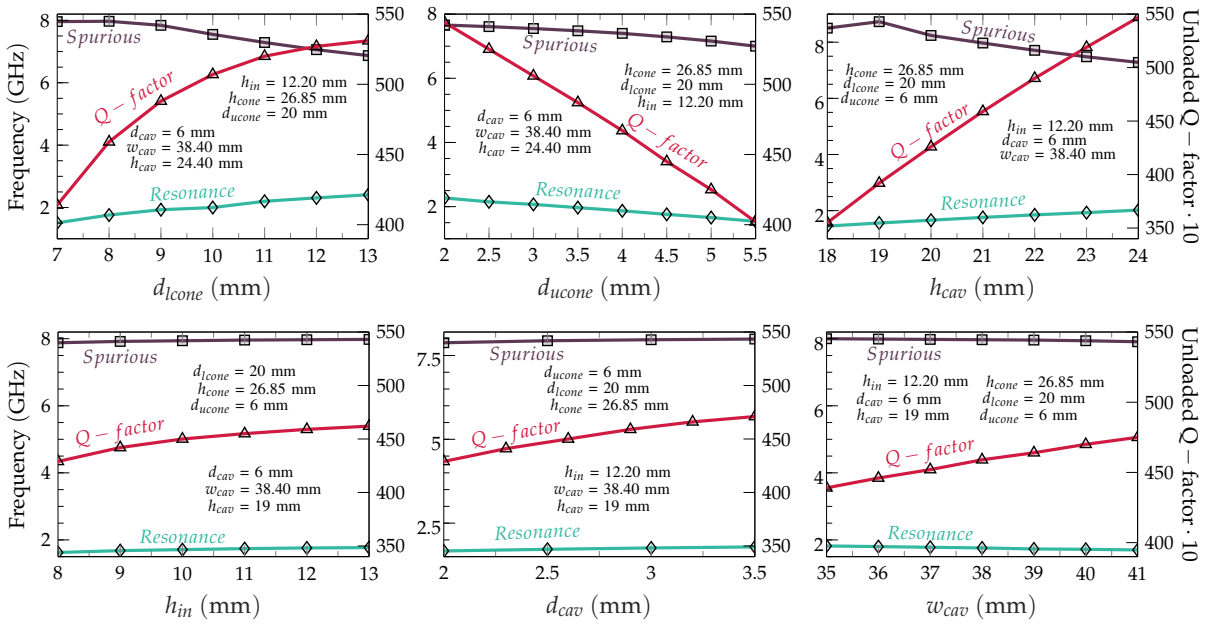

Fig. 2. Study of the different physical parameters of the conical resonator in a rectangular cavity.

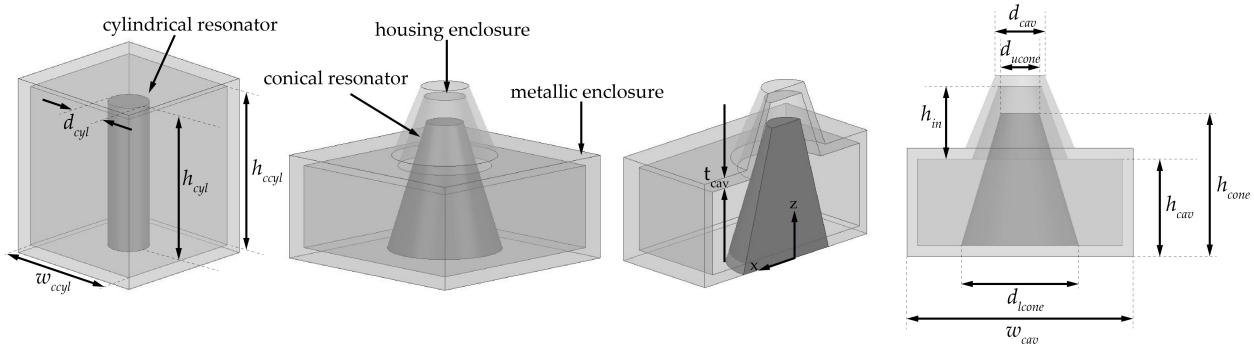

Fig. 3. 3D view of the cylindrical resonator and the proposed conical resonator. Different views.

height (h_{gap}) of the housing have less effect on the frequency, having more effect on the Q_u than the rest of the parameters. Table I and II show a brief comparison between conical post resonators and classical combline resonators. In Table I, both resonators resonate at 2.5 GHz and have a Q-factor of about 3530. In this case, the combline resonator dimensions have been taken from [27], while the dimensions of the conical resonator have been selected to obtain the same resonance frequency and Q-factor of the combline resonator. As can be seen, the conical resonator has better performances in terms of volume and spurious-free range. Indeed, the volume is 30% lower while the first spurious appears at 11.75 GHz (instead of 7.38 GHz). A wider spurious-free range is in fact achieved due to the larger capacitive loading realized by the re-entrant post (post inserted inside the cover). This principle also works for posts with non-conical shapes [28]. In Table II, both resonators resonate at 1.75 GHz and have a Q-factor of about 4650. In this case, the dimensions of the combline resonator have been selected considering a ratio between outer and inner diameter (w_{ccyl}/d_{cyl}) of 3.59. In fact, this value guarantees the minimum loss for the coaxial waveguide [29]. Also in this

TABLE I
RESONANT FREQUENCY, FIRST SPURIOUS, UNLOADED Q-FACTOR (COMPUTED FOR COPPER WITH CONDUCTIVITY σ = 58 MS/m) AND VOLUME. THE DIMENSIONS (mm) OF THE CYLINDRICAL RESONATOR ARE: w_{ccyl} = 20, h_{ccyl} = 30 , d_{cyl} = 8 AND h_{cyl} = 25; WHILE THE DIMENSIONS (mm) FROM FIG. 3 ARE: h_{cav} = 13, h_{cone} = 18.5, d_{lcone} = 12, d_{ucone} = 5, d_{cav} = 5, h_{in} = 8.2, w_{cav} = 24.7 AND t_{cav} = 2

Structure	f_{res} (GHz)	f_{spu} (GHz)	Q_u	Volume (mm^3)
Cylindrical	2.5	7.38	3530	12000
Conical	2.5	11.75	3540	8420

TABLE II
RESONANT FREQUENCY, FIRST SPURIOUS, UNLOADED Q-FACTOR (COMPUTED FOR COPPER WITH CONDUCTIVITY σ = 58 MS/m) AND VOLUME. THE DIMENSIONS (mm) OF THE CYLINDRICAL RESONATOR ARE: w_{ccyl} = 31, h_{ccyl} = 38, d_{cyl} = 8.63 AND h_{cyl} = 34; WHILE THE DIMENSIONS (mm) FROM FIG. 3 ARE: h_{cav} = 21, h_{cone} = 27.8, d_{lcone} = 14, d_{ucone} = 6, d_{cav} = 7, h_{in} = 12.2, w_{cav} = 36.7 AND t_{cav} = 1.5

Structure	f_{res} (GHz)	f_{spu} (GHz)	Q_u	Volume (mm^3)
Cylindrical	1.75	5.18	4650	36518
Conical	1.75	7.4	4650	29294

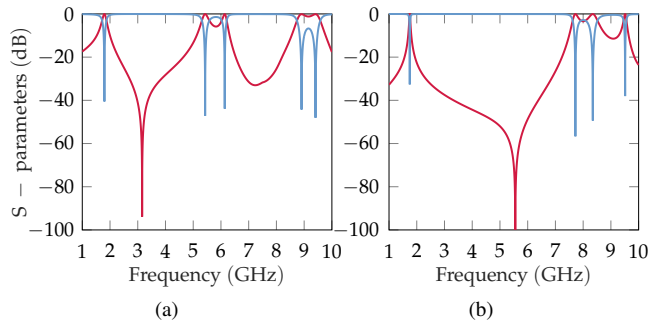

Fig. 4. S-parameters of the: (a) cylindrical resonator; (b) conical resonator. Using the dimensions from Table II.

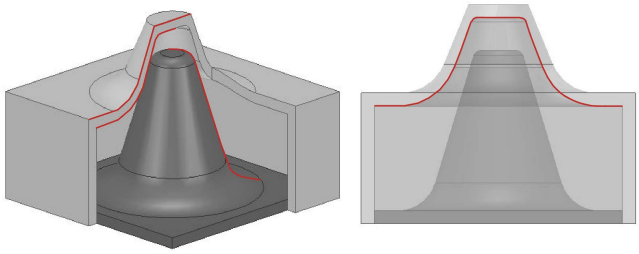

Fig. 5. Conical resonator with rounded edges.

case, the conical resonator has better performances in terms of volume and spurious-free range: the volume reduction is about 20%, whereas the first spurious appears at 7.4 GHz (instead of 5.18 GHz). Results reported in Table I and Table II have been obtained by using the eigenmode solver from the commercial software HFSS. However, according to Fig. 4, the wider spurious-free range is also confirmed considering the scattering parameters. It is worth noting that the volume performance can be further improved by rounding the housing edges and the conical post edges as shown in Fig. 5. Square corners can concentrate currents that normally entail higher losses. In order to spread the currents, round edges instead of square edges have been considered. In doing so, the Q_u of the conical resonator is increased about 4%, and in order to reobtain the initial Q_u, the cavity size can be further reduced. Another advantage of this modification is the increased space gap between the conical post and its housing. Considering rounded edges for the conical resonator in Table I, the volume reduction with respect to the combline becomes 35%. In Table II, the volume reduction becomes instead 27%, and the frequency of the spurious is at 7.2 GHz this time. Of course, the volume reductions here considered are referred to single resonators. The volume of the conical post resonator is the sum of the volume of the square cavity of height h_{cav} plus the conical bump on top of it used for housing the post. Thanks to the conical shapes, cavities can be piled. This means that the bump of a cavity is inserted into another cavity on top of it. Consequently, the bump of the first cavity is no longer contributing to the filter volume and this results in a further volume reduction with respect to the classical combline filter configuration.

III. Filter Design Procedure

The conical resonator presented in Section II can be used to design higher order filters. In [26], the procedure to design a 2-pole filter was briefly described. The first step consists in the evaluation of the coupling (k) and external quality factor (Q_e) of the equivalent circuit. The second step consists in the evaluation of the physical dimensions of the filter that realizes the prescribed k and Q_e. This is done by using diagrams obtained through full-wave simulations. The equivalent circuit representation of a 4-pole bandpass filter, based on coupled-series resonators is shown in Fig. 6.

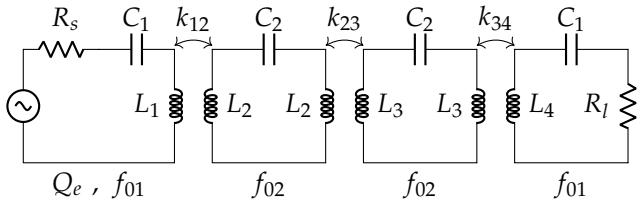

Fig. 6. Equivalent circuit representation of a 4-pole filter based on series of inductive interresonator coupling.

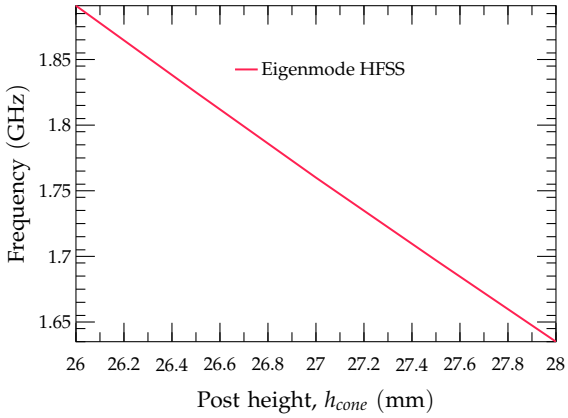

Fig. 7. Frequency versus the height of the conical post.

In addition to the vertical arrangement proposed in [26], horizontal arrangements are also possible (see Fig. 8). This leads to more interesting solutions with mixed vertical/horizontal arrangements, as will be shown later on. In this section, the design procedure of a 3-pole (3 x 1) filter consisting of 3 piled cavities, and a 4-pole (2 x 2) filter consisting of two piled cavities horizontally connected to others two piled cavities are described. The filter design starts with a preliminary design of the resonators. In this case, all filters are working at 1.75 GHz. This means that we can use this preliminary design for all resonators of all filters here considered. According to Fig. 3, cavity dimensions are: h_{cav} = 19 mm; w_{cav} = 38 mm; d_{ucone} = 6.8 mm; d_{lcone} = 17.2 mm, d_{cav} = 6.8 mm and h_{in} = 12.8 mm. The resonance frequency is determined by h_{cone}. The initial value for h_{cone} = 27.07 mm is obtained by using the diagram of Fig. 7. The input and output of the filter will be fed through two coaxial cables united to a metallic connector that is attached to the conical posts (Fig. 8). The Q_e value provided by an input coupling structure is evaluated as follows:

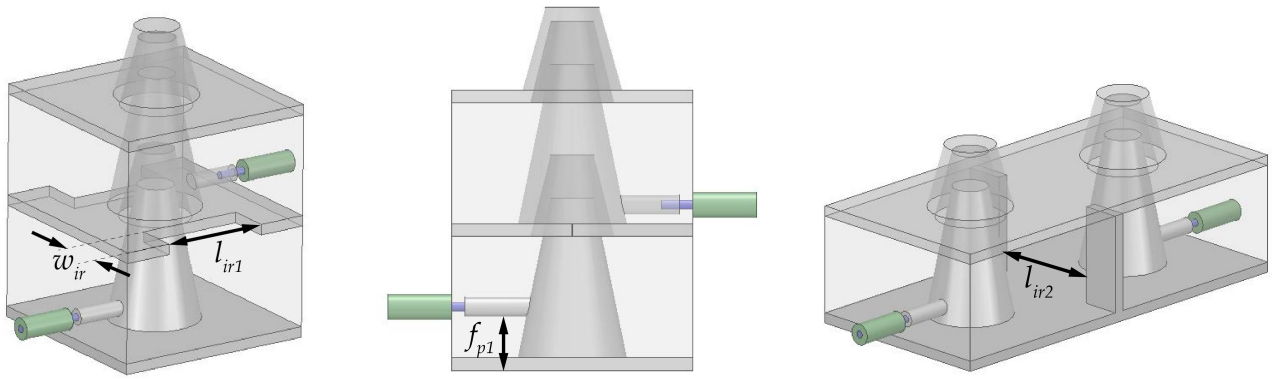

(a) (b) (c)

Fig. 8. Doublet filter: (a) vertical structure with a low input/output position (f_{p1}) to weakly excite the structure; (b) vertical structure with closed apertures for computing the external Q-factor; (c) horizontal structure.

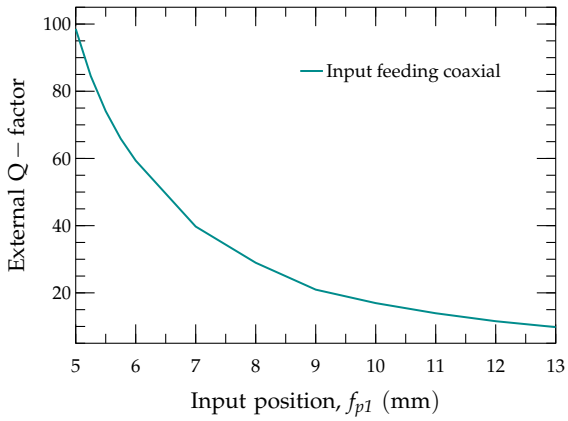

Fig. 9. External Q-factor versus the coaxial feeding position (f_{p1}).

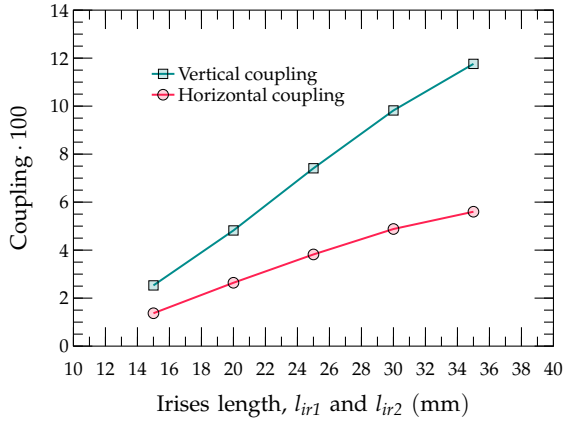

Fig. 10. Coupling coefficients versus the length of the irises (l_{ir1} and l_{ir2}). For computing the coupling related to l_{ir1}, the value of w_{ir} is equal to 10 mm.

$$Q_e = \frac{\omega_0}{\Delta\omega_{\pm 90^\circ}} \tag{1}$$

Where ω_0 is the resonance frequency of the considered structure; and $\Delta\omega$ is the difference between the two angular frequencies, where the phase of the S_{21} parameters is shifted, respectively, $\pm 90^\circ$ with respect to the phase value at ω_0. In Fig. 9, the diagram for the estimation of Q_e as a function of the input position is shown. According to Fig. 8(a), for the implementation of the coupling between adjacent vertically arranged cavities, two apertures placed sideways connecting the two cavities have been exploited. In case of horizontally arranged cavities instead, a single aperture in the wall separating the two cavities has been used (Fig. 8(c)). In Fig. 10, a diagram for the estimation of the coupling k between adjacent cavities as a function of the aperture sizes is shown. The graph contains two curves: one is for the horizontal and the other is for the vertical arrangement. The two curves have been obtained by considering the frequencies f_1 and f_2 of the two reflection zeros of a 2-pole filter response with very high Q_e and applying the formula:

$$k = \frac{f_2^2 - f_1^2}{f_2^2 + f_1^2} \tag{2}$$

A. Frequency correction

When coupling apertures or input couplings are considered, the resonant frequency of the cavities changes. In order to recover the original resonance frequency, two procedures are suggested. The first procedure is applicable to the input/output cavities of the filters (the first and the last cavity). The second to all the others (internal cavities).

Input/output cavities: Supposing is the first cavity resonance to be readjusted, the first two cavities of the filter (implementing a doublet) shall be considered. The aperture between the two cavities shall be that estimated by using Fig. 10, while both input and output height f_{p1} shall be equal to the value estimated for the cavity 1 by using Fig. 9. Resonator 2 shall then be detuned. This can be done by increasing the post height until reaching the ceiling of the housing enclosure (see Fig. 11 inset). The response of this structure, because of the detuning of resonator 2, is now a single-pole response. The readjusted height of the first cavity post can be found just restoring the resonance of the single-pole response (1.75 GHz in this case). Same procedure can be followed for readjusting the resonance frequency of the last cavity.

Internal cavities: This is the case of all resonators except first and last. In that case, the triplet consisting of the n^{th}

cavity (the one to be tuned) together with its adjacent cavities ($(n-1)^{th}$ and $(n+1)^{th}$) is considered. Cavities $(n-1)^{th}$ and $(n+1)^{th}$ shall be connected to an input and an output, and then detuned by increasing the post height until reaching the ceiling, as shown in the inset of Fig. 11 for the case of 3 vertically positioned cavities. Certainly, the same method can be applied for horizontally or mixed vertically and horizontally arranged cavities. The resulting response is a single-pole response. The readjusted height of the post of the n^{th} cavity can be found just restoring the resonance of the single-pole response to the original frequency (1.75 GHz in this case).

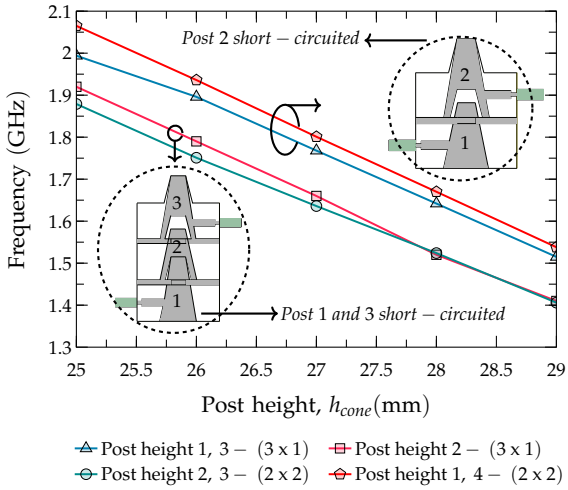

Fig. 11. Curves of the frequency deviation versus height of the posts.

B. 3-order filter (3 x 1 configuration)

The filter to be designed is a 3-order filter centered at 1.75 GHz with a fractional bandwidth (FBW) of 5%. In Fig. 12 and Fig. 13, the structure of the filter and its relevant routing scheme are shown, respectively. The Chebyshev synthesis leads to the following values of the coupling coefficients k_{S1} = k_{3L} = 0.22, k_{12} = k_{23} = 0.045. According to the formula defined in (3) this corresponds to an external Q-factor

$$Q_e = \frac{1}{k_{S1}^2} = 20.66 \tag{3}$$

As indicated previously, the first step of the design consists in the preliminary design of the conical posts resonating at 1.75 GHz, which corresponds, in agreement with Fig. 7, to a post height h_{cone} = 27.07 mm. According to the diagram of Fig. 9, the external Q-factor Q_e = 20.66 is realized with a position f_{p1} = 9.15 mm and f_{p2} = 9.15 mm of input and output coaxial feeding probes, respectively. According to the curve related to the vertical coupling in the diagram of Fig. 10, the coupling k_{12} = 0.045 is realized by apertures with l_{ir1} = l_{ir2} = 19.59 mm.

Input/output couplings and coupling apertures perturb the resonant mode of the cavities that can be retuned by following the procedures of the previous subsection. Curves in Fig. 11 have been obtained by following those procedures and show the resonant frequency of the single-pole response as a function of the post height. In particular, considering the post height 1 and 3 curves related to h_{cone1} and h_{cone3}, it can be seen that the resonance frequency is restored at 1.75 GHz

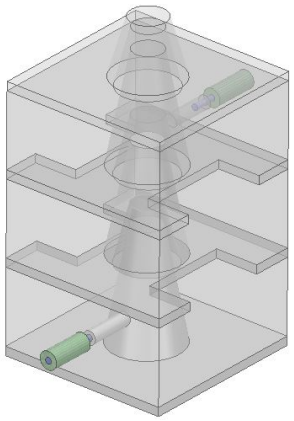

Fig. 12. 3D view of the 3-pole filter (3 x 1).

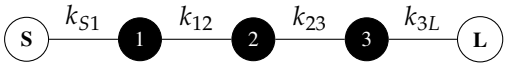

Fig. 13. Routing scheme of the 3-pole filter.

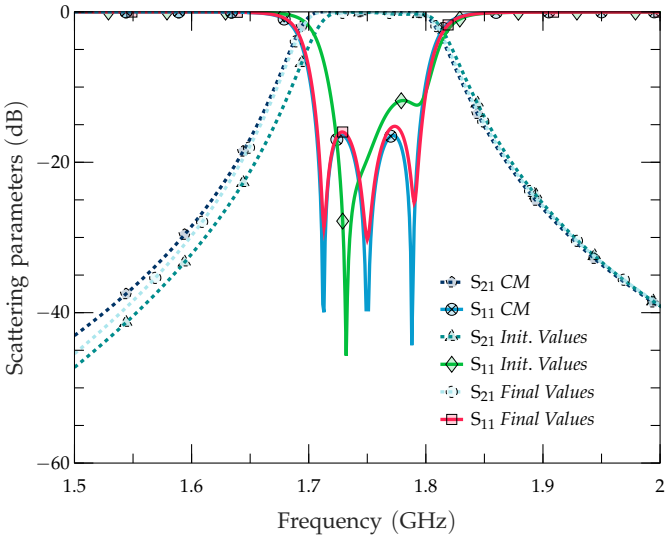

Fig. 14. Ideal and simulated responses (S-parameters) of the considered 3-pole filter.

TABLE III
DIMENSIONS OF THE 3-POLE FILTER WITH FBW OF 5%, VALUES OF THE COUPLING MATRIX: k_{s1} = 0.22, k_{12} = 0.045

Elec. Par.	Value	Phys. Par.	Init. Value	Final Value
f_{01}	1.75	h_{cone1}	27.1	27.21
f_{02}	1.75	h_{cone2}	26.28	26.3
f_{01}	1.75	h_{cone3}	27.1	26.98
Q_e	20.66	f_{p1}	9.15	9.5
Q_e	20.66	f_{p2}	9.15	8.7
k_{12}	0.045	l_{ir1}	19.59	19.8
k_{23}	0.045	l_{ir2}	19.59	20.8

when $h_{cone1} = h_{cone3} = 27.1$ mm. Considering instead the post height 2 curve, the value of $h_{cone2} = 26.28$ mm restores the frequency at 1.75 GHz. The values of the input positions, the aperture sizes and the retuned h_{cone} values are summarized in Table III in the column 'Init. Value'. In Fig. 14, the full-wave simulation of the filter obtained with the initial values is shown along with the ideal coupling matrix response and the response after the filter has been optimized. As can be seen, the starting point is quite good. The filter dimensions after the optimization are summarized in Table III in the column 'Final Value'. As can be noted, the final value of l_{ir1} and l_{ir2}, as well as f_{p1} and f_{p2} are slightly different. This is due to the fact that the physical structure is not completely symmetric.

C. 4-pole filter (2 x 2 Configuration)

The filter to be designed is a 4-order filter centered at 1.75 GHz with FBW of 7%. In Fig. 15 and Fig. 16, the structure of the filter and its relevant routing scheme are shown, respectively. The Chebyshev synthesis leads to the following values of the coupling coefficients $k_{S1} = k_{4L} = 0.2687$, $k_{12} = k_{34} = 0.0665$ and $k_{23} = 0.0526$. According to the equation (3), $Q_e = 13.85$. Analogously to the 3-order filter, the preliminary design of conical posts leads to a post height $h_{cone} = 27.07$ mm. In agreement with the diagram of Fig. 9, the external Q-factor $Q_e = 13.85$ is realized with a position $f_{p1} = f_{p2} = 11.03$ mm of input and output coaxial. According to the curve related to the vertical coupling in the diagram of Fig. 10, the coupling $k_{12} = k_{34} = 0.0665$ is realized by an aperture with $l_{ir1} = 23.5$ mm, while for the curve related to the horizontal coupling in the diagram of Fig. 10, the coupling $k_{23} = 0.0526$ is realized by an aperture with $l_{ir2} = 32.1$ mm. In accordance with the 3-order filter, Fig. 11 can be used to retune the cavities after the input/output couplings and the coupling apertures are considered. In particular, considering the post height 1 and 4 curve related to h_{cone1} and h_{cone4}, it can be seen that the resonance frequency is restored at 1.75 GHz when $h_{cone1} = h_{cone4} = 27.38$ mm. Considering instead the post height 2 and 3 curves, the value of $h_{cone2} = h_{cone3} = 26$ mm restores the frequency at 1.75 GHz. The values of input positions, aperture sizes and retuned h_{cone} values are summarized in Table IV in the column 'Init. Value'. In Fig. 17, the full-wave simulation of the filter obtained with the initial values are shown along with the ideal coupling matrix response and the response after the filter has been optimized. As can be seen, the starting point is even better than that of the 3-order filter. The filter dimensions after the optimization are summarized in Table IV in the column 'Final Value'.

D. Tuning

Tuning capability is a desired feature in filtering structures, as it allows the mitigation of problems related to manufacturing tolerances. In the classical combline filters, tuning screws are generally placed in the ceiling in correspondence of the top of the posts. This position is not always possible in the proposed structures, as cavities can be piled. For this reason, three different possible locations are considered:

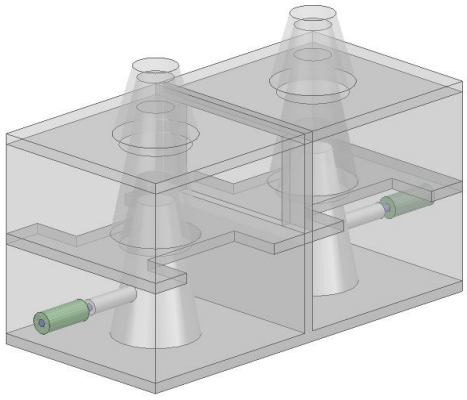

Fig. 15. 3D view of the 4-pole filter (2 x 2).

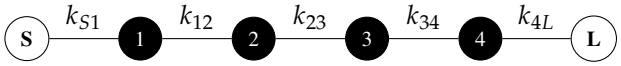

Fig. 16. Routing scheme of the 4-pole filter.

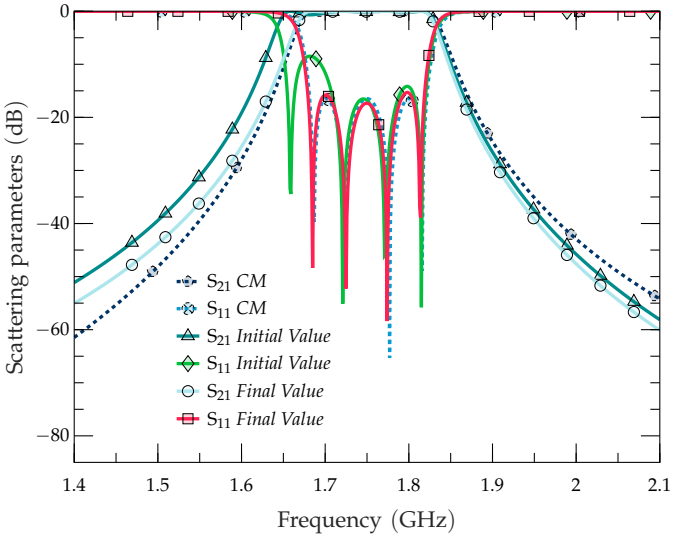

Fig. 17. Ideal and simulated responses (S-parameters) of the considered 4-pole filter.

TABLE IV
DIMENSIONS 4-POLE FILTER WITH FBW OF 7%, VALUES OF THE COUPLING MATRIX: $k_{s1} = 0.2687$, $k_{12} = 0.0665$ AND $k_{23} = 0.0526$

Elec. Par.	Value	Phys. Par.	Init. Value	Final Value
f_{01}	1.75	h_{cone1}	27.38	27.42
f_{02}	1.75	h_{cone2}	26	26.07
Q_e	13.85	f_{p1}	11.03	11.03
k_{12}	0.0665	l_{ir1}	23.5	22.45
k_{23}	0.0526	l_{ir2}	32.1	27.80

1) **At the top of the conical enclosure**: This position is realizable for cavities that have not other cavities on their top. Two examples are screws 2 and 3 of Fig. 18(a).
2) **Inside the conical post**: This position is possible for cavities that are not positioned on top of other cavities. The resonance frequency can be tuned by inserting a

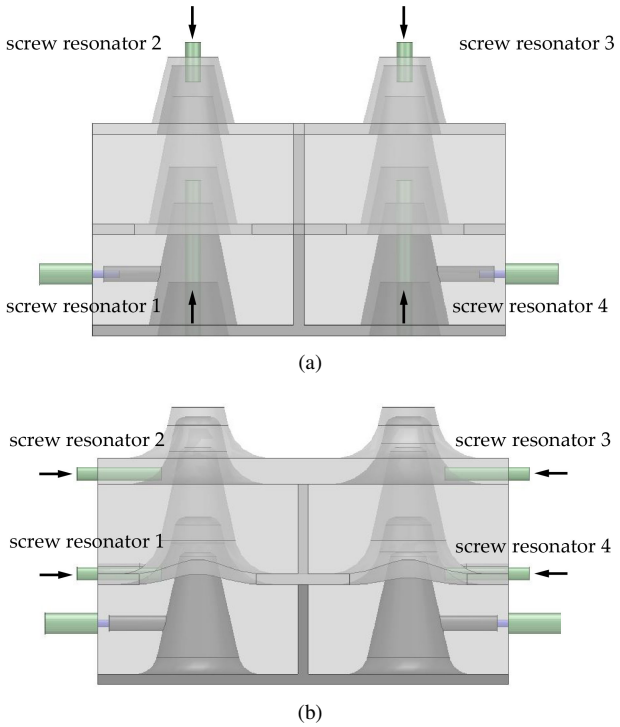

Fig. 18. 3D view of conical post filters: (a) 4-pole filter using screws vertically; (b) 4-pole filter with rounded edges using screws horizontally.

screw through the conical post from the bottom of the structure. Two examples are screws 1 and 4 of Fig. 18(a).

3) **Inside the septum between two piled cavities**: This position is allowed even for cavities having a cavity on its top and on its bottom. In Fig. 18(b), examples of that screw positioning are shown. Considering that usually the septum separating two cavities is very small and cannot house a screw, a bump above the septum is created, increasing the thickness of a small area of the septum as shown in Fig. 18(b) and Fig. 19.

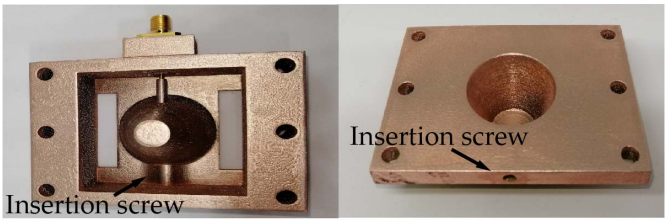

Fig. 19. A doublet filter with a small bump for tuning the response using screws horizontally [26].

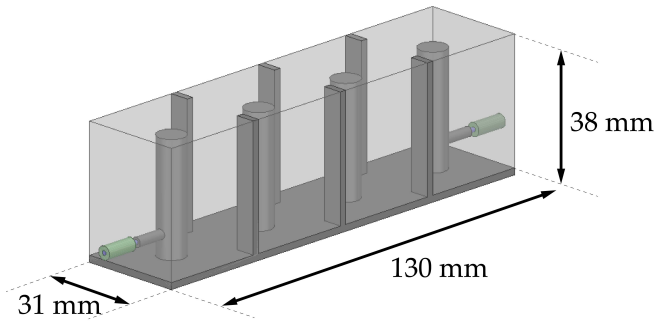

Fig. 20. 3D view of the 4-pole combline filter.

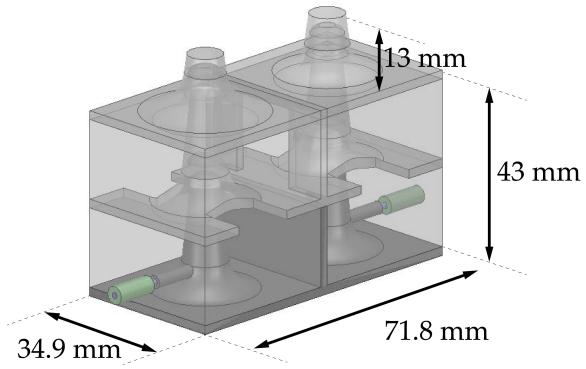

Fig. 21. 3D view of the 4-pole conical filter.

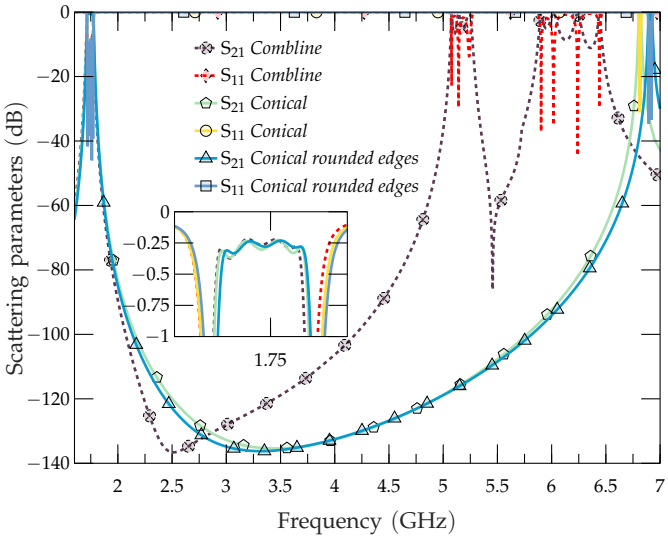

Fig. 22. Wideband response of the 4-pole filter centered at 1,75 GHz with 48 MHz bandwidth. Comparison among conical post filters (with and without rounded edges) and classical combline filter. In the figure inset, the in-band insertion loss is also shown.

E. Comparison with a conventional combline filter

4-pole filters centered at f_0 = 1.75 GHz with FBW of 2.7% have been designed in both combline technology and conical resonator technology for comparison purposes. For both combline and conical resonator filters, the selected resonators are those already compared in Table II with a nominal Q-factor of 4650. The combline filter geometry is shown in Fig. 20. In addition to the version with non-rounded edges, a conical resonator filter with rounded edges (sketched in Fig. 21) has been also designed. In Fig. 22, the responses of the designed filters are shown. The Q-factor of the filters extracted from their responses is, as expected, lower than the nominal one and it is about 3500 for all the three filters. As can be seen, conical resonator filters present a wider spurious-free band. In particular, the first spurious appears at $3.9 \cdot f_0$, this leading to a spurious-free band of about 5.1 GHz. Only a difference of about 100 MHz in the spurious-free band is observed between

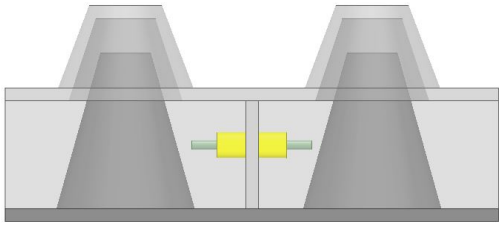

Fig. 23. Bottom part of the structure connecting the first and last resonators using semirigid coaxial cable between the two non-adjacent resonators.

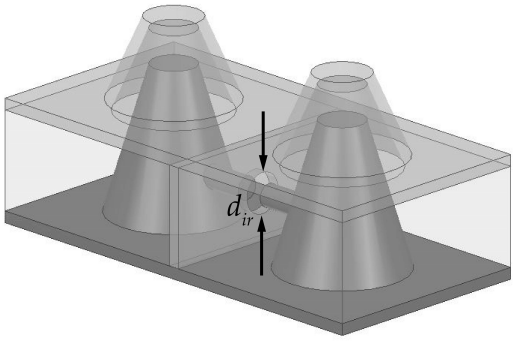

(a)

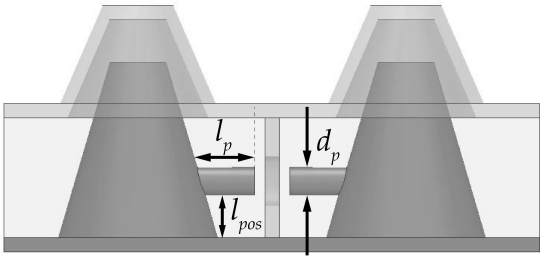

(b)

Fig. 24. Bottom part of the structure connecting the first and last resonators with one electric probe attached to each resonator.

the version with and without rounded edges. The first spurious of the combline filter appears instead at $2.8 \cdot f_0$, corresponding to a spurious-free band of 3.25 GHz. With respect to the combline, the length of the conical resonator filter is about 45% shorter, while the volume reduction is 29%.

F. Transmission zeros

Mixed horizontal and vertical configurations permit couplings between non-adjacent cavities. This allows for the introduction of TZs in the filter response. However, for the generation of TZs, it is necessary to generate negative couplings. Some solutions implemented in coaxial cavity filters entail the use of a metallic probe held by a plastic material that works as a support or the use of a semirigid coaxial cable between non-adjacent resonators providing a capacitive coupling [30]. The latter, has been simulated and has proven to be a viable solution for obtaining more selective responses. Fig. 23 shows a coupling structure consisting of a semirigid coaxial cable that is close to both resonators.

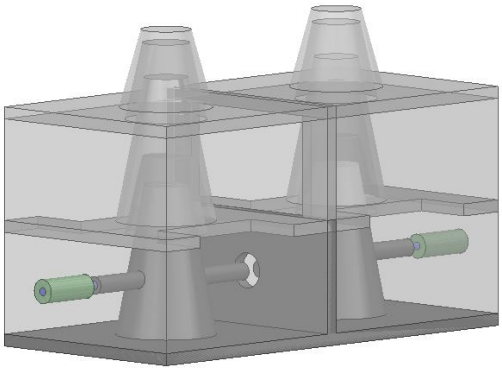

Fig. 25. 3D view of the 4-pole filter (2 x 2) with electric probes attached to resonators 1 and 4.

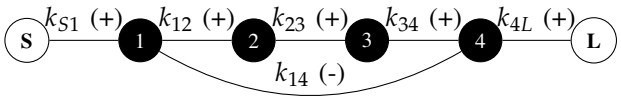

Fig. 26. Routing scheme of the 4-pole filter with cross-coupling between resonators 1 and 4.

Considering a 4-pole filter, the main couplings for paths 1-2-3-4 are based on the magnetic field (inductive couplings), whereas the cross-coupling between resonators 1-4 is based on the electric field (capacitive coupling). This creates a negative coupling that generates TZs both above and below the passband. In this case, the parameters that change the cross-coupling are the length and the position of the coaxial cable. By exploiting the AM flexibility, it is possible to use alternative coupling structures that cannot be manufactured (or would be hardly manufactured) by using traditional techniques. An example can be seen in Fig. 24, where each conical post has a probe attached. The two probes face each other through a circular hole in the septum dividing the two cavities. This structure is capable of a negative coupling. In Fig. 25. its application to a 4-order filter is shown. That filter implements the routing scheme of Fig. 26. On the other hand, Figs. 27, 28, 29 and 30 show the variation of the response of the filter of Fig. 25 as a function of some parameters of the negative coupling section. Parameters are shown in Fig. 24. When increasing the diameter of the iris (d_{ir}), it can be seen that the TZ located at higher frequencies barely changes, whereas the TZ at lower frequencies decreases. Furthermore, it can be noted that the TZ below the passband is no longer visible when increasing d_{ir}. If we increase the position of the electric probes (l_{pos}), both TZs get closer to the passband of the filter. Similarly, the length of the probe (l_p) and the diameter of the probe (d_p) have similar effects, with the generated TZs moving closer to the passband when increasing both physical parameters.

IV. 3D-Printed Filter Prototyping

A 4-pole filter (2 x 2) was manufactured and measured. The resulting component was divided into three different parts that were manufactured individually: the base formed by the first and last cavities, the top level formed by the second and third

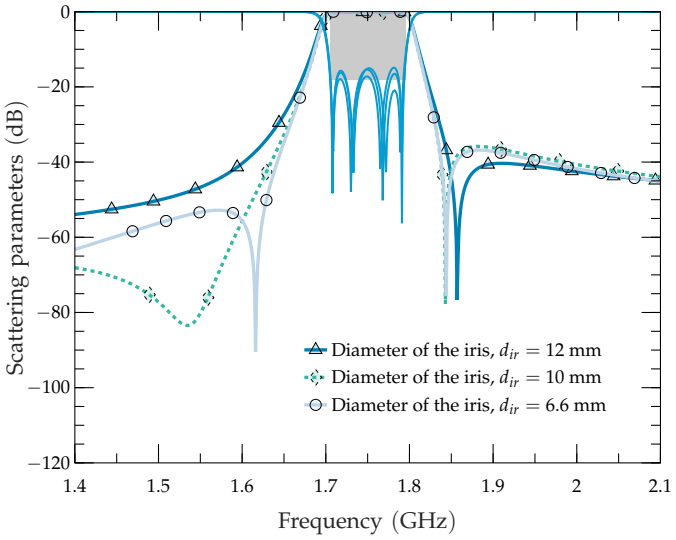

Fig. 27. Simulated responses (S-parameters) of the 4-pole bandpass filter changing the diameter of the iris.

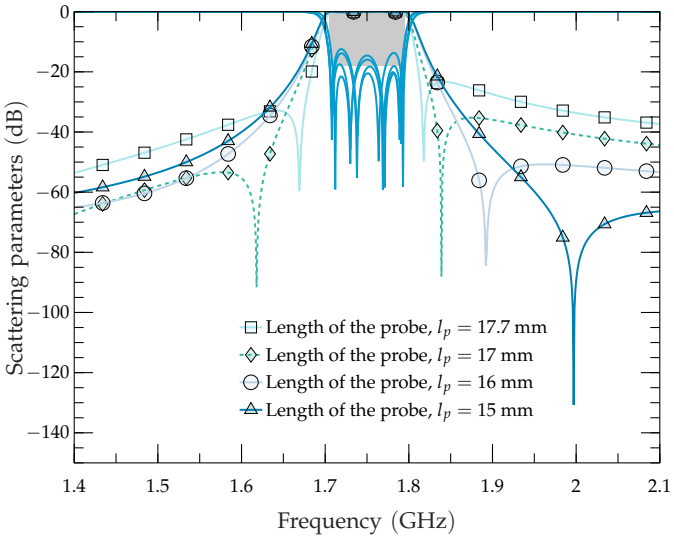

Fig. 29. Simulated responses (S-parameters) of the 4-pole bandpass filter changing the length of the electric probes.

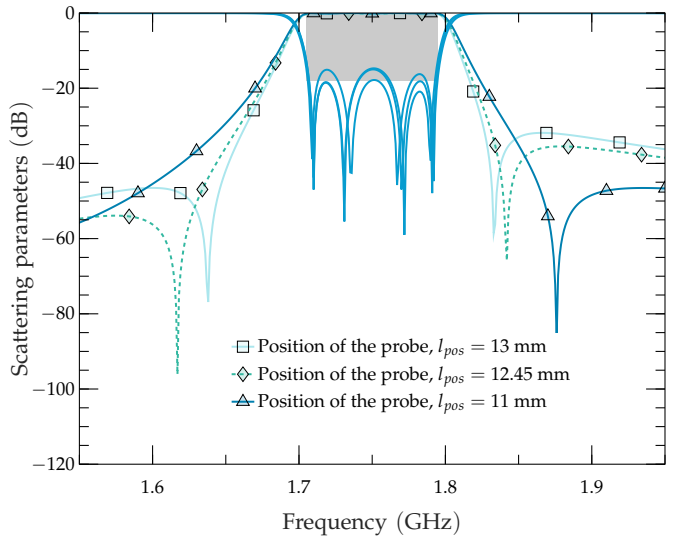

Fig. 28. Simulated responses (S-parameters) of the 4-pole bandpass filter changing the position of the electric probes.

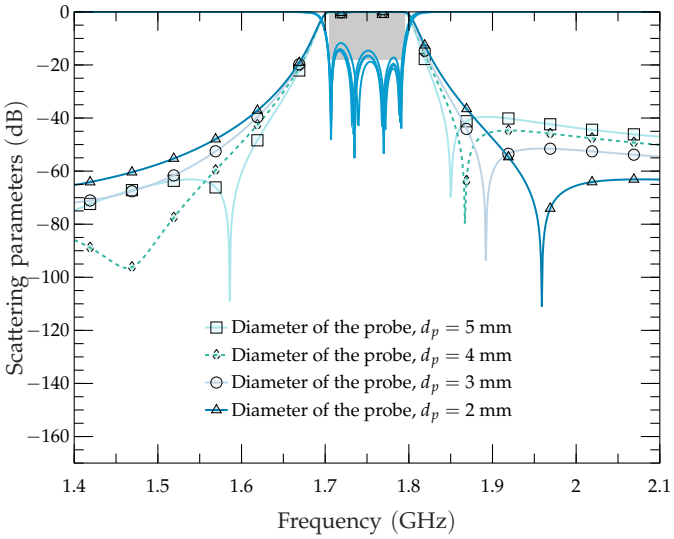

Fig. 30. Simulated responses (S-parameters) of the 4-pole bandpass filter changing the diameter of the electric probes.

cavities, and the last part is the lid formed by the enclosures that are also exploited for housing the second and the third resonator. The three parts were fabricated using a 3D printer, in particular, a Stratasys Objet 260 Connex 3 printer, based on the technique called Polyjet technology and belonging to the class of material jetting technologies. This type of technology works by jetting thousands of photopolymer droplets onto a build platform and solidifying them with a UV lamp [31]. The technology employed has one of the highest dimensional accuracies achievable among 3D-printed technologies, except only the two-photon polymerization technique which is capable of reaching nanometer resolution, but which has also a very limited building volume, not compatible with the component dimensions. The 3D printing material employed in this study is the VeroCyan photopolymer, so a metallization process was carried out by adopting the electroplating technique (copper has been used). The different parts can be observed in Fig. 31. The filter has been assembled by means of several screws at the external borders of the structure.

The specifications of the filter along with the final dimensions of the filter can be seen in Table IV. The obtained Q-factor (computed for copper with conductivity σ = 58 MS/m, and including aluminum tuning screws with conductivity σ = 33 MS/m) from the response is 2400. Fig. 32 shows the comparison between the simulation and the measurement. The minimum measured insertion loss is 1.3 dB, as opposed to the 0.15 dB of the simulation. The minimum return loss is about 16 dB. There is a small frequency shift due to the fabrication tolerances. Because of the limited tuning range of the tuning screws, this frequency shift cannot be recovered. However better results can be obtained by using horizontal tuning screws instead of the vertical ones used in this prototype.

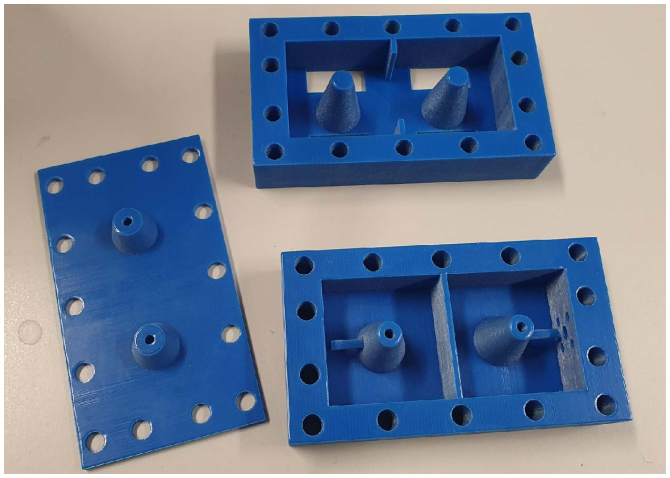

Fig. 31. Different 3D-printed parts of a 4-pole filter (2 x 2) before the metallization.

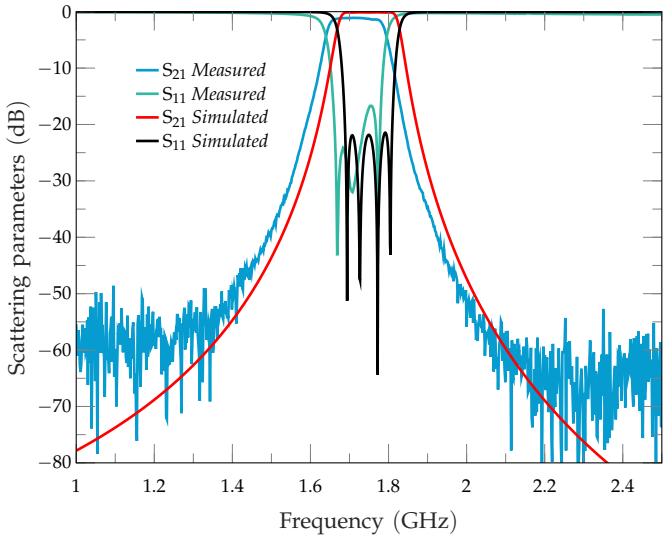

Fig. 32. Simulated and measured responses (S-parameters) of the proposed filter.

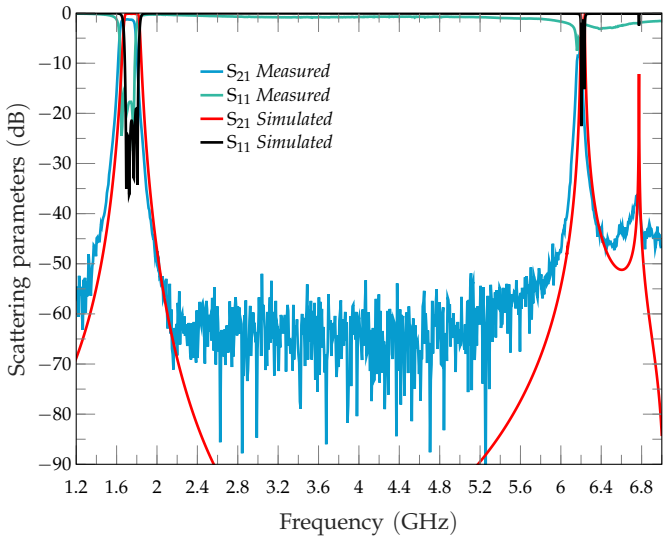

Fig. 33. Simulated and measured responses (S-parameters) in a wide-frequency band (up to 7 GHz) of the proposed filter.

Indeed, horizontal tuning screws exhibit a wider tuning range. Fig. 33 also shows the scattering parameters over a wide-frequency range. It can be seen that the frequency shift has also affected the out-of-band performance. Nevertheless, the agreement is good both, in the in-band and in the out-of-band rejection.

V. Conclusion

Different configurations of bandpass filters based on conical resonators have been presented. The resonator has a conical post that is slightly inserted in a hollowed housing enclosure that has the same external dimensions as the conical post. Such implementation can be used as an alternative to classical combline filters, providing more compact structures that reduce the overall volume of the filters while providing different footprints due to various configurations (vertically and/or horizontally). In addition to this, the proposed filter provides better out-of-band rejections than the traditional combline filter configuration with non-re-entrant posts, and enhanced responses are possible thanks to cross-couplings between non-adjacent resonators. The design procedure of two filters with different configurations ((3 x 1) and (2 x 2)) has been explained in this paper, and for validation purposes, a 4-order filter prototype (with 7% of relative bandwidth, and a central frequency of 1.75 GHz) has been designed and manufactured using a 3D printer, and then plated. The prototype has been tested proving the viability of the proposed filter using additive manufacturing techniques.

References

[1] A. E. Williams, "A four-cavity elliptic waveguide filter," *IEEE Transactions on Microwave Theory and Techniques*, vol. 18, no. 12, pp. 1109–1114, December 1970.

[2] R. R. Bonetti and A. E. Williams, "A TE triple-mode filter," in *1988., IEEE MTT-S International Microwave Symposium Digest*, 1988, pp. 511–514 vol.1.

[3] U. Rosenberg, S. Amari, and J. Bornemann, "Inline TM_{110}-mode filters with high-design flexibility by utilizing bypass couplings of nonresonating $TE_{10/01}$ modes," *IEEE Transactions on Microwave Theory and Techniques*, vol. 51, no. 6, pp. 1735–1742, June 2003.

[4] S. Bastioli, C. Tomassoni, and R. Sorrentino, "A new class of waveguide dual-mode filters using TM and nonresonating modes," *IEEE Transactions on Microwave Theory and Techniques*, vol. 58, no. 12, pp. 3909–3917, Dec. 2010.

[5] S. Bastioli, and C. Tomassoni, and R. Sorrentino, "TM dual-mode pseudoelliptic filters using nonresonating modes," in *2010 IEEE MTT-S International Microwave Symposium*, Anaheim, CA, May 2010, pp. 880–883.

[6] C. Tomassoni, S. Bastioli, and R. Sorrentino, "Generalized TM dual-mode cavity filters," *IEEE Transactions on Microwave Theory and Techniques*, vol. 59, no. 12, pp. 3338–3346, Dec. 2011.

[7] C. Wang and K. A. Zaki, "Dielectric resonators and filters," *IEEE Microwave Magazine*, vol. 8, no. 5, pp. 115–127, Oct. 2007.

[8] S. J. Fiedziuszko and S. Holmes, "Dielectric resonators raise your high-Q," *IEEE Microwave Magazine*, vol. 2, no. 3, pp. 50–60, Sept. 2001.

[9] R. R. Mansour, "High-Q tunable dielectric resonator filters," *IEEE Microwave Magazine*, vol. 10, no. 6, pp. 84–98, Oct. 2009.

[10] L. Pelliccia, F. Cacciamani, C. Tomassoni, and R. Sorrentino, "Ultra-compact filters using TM dual-mode dielectric-loaded cavities with asymmetric transmission zeros," in *2012 IEEE/MTT-S International Microwave Symposium Digest*, Montreal, QC, June 2012, pp. 1–3.

[11] S. B. Cohn, "Microwave bandpass filters containing high-Q dielectric resonators," *IEEE Transactions on Microwave Theory and Techniques*, vol. 16, no. 4, pp. 218–227, April 1968.

[12] C. Tomassoni, S. Bastioli, and R. V. Snyder, "Propagating waveguide filters using dielectric resonators," *IEEE Transactions on Microwave Theory and Techniques*, vol. 63, no. 12, pp. 4366–4375, Dec. 2015.

[13] C. Tomassoni, S. Bastioli, and R. V. Snyder, "Compact mixed-mode filter based on TE_{101} cavity mode and $TE_{01\delta}$ dielectric mode," *IEEE Transactions on Microwave Theory and Techniques*, vol. 64, no. 12, pp. 4434–4443, Dec. 2016.

[14] L. Pelliccia, F. Cacciamani, C. Tomassoni, and R. Sorrentino, "Ultra-compact pseudoelliptic waveguide filters using TM dual-mode dielectric resonators," in *Asia-Pacific Microwave Conference 2011*, Melbourne, VIC, 2011, pp. 143–146.

[15] G. L. Matthaei, "Combline band-pass filters of narrow or moderate bandwidth," *Microwave J.*, vol. 6, Aug. 1963.

[16] Hui-Wen Yao, K. A. Zaki, A. E. Atia, and R. Hershtig, "Full wave modeling of conducting posts in rectangular waveguides and its applications to slot coupled combline filters," *IEEE Transactions on Microwave Theory and Techniques*, vol. 43, no. 12, pp. 2824–2830, Dec 1995.

[17] Y. Wang and M. Yu, "True inline cross-coupled coaxial cavity filters," *IEEE Transactions on Microwave Theory and Techniques*, vol. 57, no. 12, pp. 2958–2965, Dec 2009.

[18] M. Hoft and F. Yousif, "Orthogonal coaxial cavity filters with distributed cross-coupling," *IEEE Microwave and Wireless Components Letters*, vol. 21, no. 10, pp. 519–521, Oct 2011.

[19] R. Tkadlec and G. Macchiarella, "Pseudoelliptic combline filter in a circularly shaped tube," in *2018 IEEE/MTT-S International Microwave Symposium - IMS*, Philadelphia, PA, 2018, pp. 1099–1102.

[20] R. V. Snyder and S. Bastioli, "Transmission zero generation for wide-band high frequency evanescent mode filters," in *2014 IEEE MTT-S International Microwave Symposium (IMS2014)*, Tampa, FL, 2014, pp. 1–4.

[21] C. Tomassoni and R. Sorrentino, "A new class of pseudo-elliptic waveguide filters using resonant posts," in *2012 IEEE/MTT-S International Microwave Symposium Digest*, Montreal, QC, 2012, pp. 1–3.

[22] F. Gentili, L. Pelliccia, R. Sorrentino, and G. Bianchi, "High Q-factor compact filters with wide-band spurious rejection," in *2012 42nd European Microwave Conference*, Amsterdam, 2012, pp. 160–163.

[23] C. Tomassoni, G. Venanzoni, M. Dionigi, and R. Sorrentino, "Compact quasi-elliptic filters with mushroom-shaped resonators manufactured with 3-d printer," *IEEE Transactions on Microwave Theory and Techniques*, vol. 66, no. 8, pp. 3579–3588, Aug. 2018.

[24] G. Venanzoni, M. Dionigi, C. Tomassoni, and R. Sorrentino, "3-d-printed quasi-elliptical evanescent mode filter using mixed electromagnetic coupling," *IEEE Microwave and Wireless Components Letters*, vol. 28, no. 6, pp. 497–499, June 2018.

[25] E. Doumanis, L. Guan, G. Goussetis, and D. Ferling, "Dual-band bandpass double ground plane coaxial resonators and filters," *IEEE Transactions on Microwave Theory and Techniques*, vol. 66, no. 8, pp. 3828–3835, Aug. 2018.

[26] E. López-Oliver, C. Tomassoni, L. Silvestri, M. Bozzi, L. Perregrini, S. Marconi, G. Alaimo, and F. Auricchio, "3-d printed bandpass filter using conical posts interlaced vertically," in *2020 IEEE/MTT-S International Microwave Symposium - IMS*, Los Angeles, CA, 2020, pp. 580–582.

[27] D. Sh-Asanjan and R. R. Mansour, "A novel coaxial resonator for high power applications," in *2014 44th European Microwave Conference*, Rome, 2014, pp. 295–298.

[28] S. Bastioli and R. V. Snyder, "Evanescent mode filters using strongly-coupled resonator pairs," in *2013 IEEE MTT-S International Microwave Symposium Digest (MTT)*, Seattle, WA, 2013, pp. 1–3.

[29] M. Hoft, T. Magath, O. Bartz, and S. Burger, "Corner rounding for increased quality factor of cavity resonators," in *2005 Asia-Pacific Microwave Conference Proceedings*, vol. 1, Suzhou, 2005, pp. 4 pp.–.

[30] J. B. Thomas, "Cross-coupling in coaxial cavity filters - a tutorial overview," *IEEE Transactions on Microwave Theory and Techniques*, vol. 51, no. 4, pp. 1368–1376, April 2003.

[31] F. Hsieh, P. Lin, H. Pan, C. Yu, C. Chang, and Y. Hu, "Mechanical behavior of photopolymer for additive manufacturing applications," in *2017 IEEE International Instrumentation and Measurement Technology Conference (I2MTC)*, Turin, 2017, pp. 1–4.